

RESEARCH ARTICLE

10.1002/2015GC006118

Persistent multitiered magma plumbing beneath Katla volcano, Iceland

David A. Budd¹, Valentin R. Troll¹, Börje Dahren¹, and Steffi Burchardt¹¹Centre for Experimental Mineralogy, Petrology and Geochemistry, Department of Earth Sciences, Uppsala University, Uppsala, Sweden

Key Points:

- Mineral-melt thermobarometry on age-constrained tephra layers reveals information on Katla's magma plumbing system.
- Evidence for the last 8 kyr suggests persistent deep and shallow crustal magma storage.
- Replenishment of shallow magma pockets could possibly lead to Eyjafjallajökull-style ash eruptions.

Supporting Information:

- Supporting Information S1
- Data Set S1
- Data Set S2
- Data Set S3
- Data Set S4

Correspondence to:

V. R. Troll,
valentin.troll@geo.uu.se

Citation:

Budd, D. A., V. R. Troll, B. Dahren, and S. Burchardt (2016), Persistent multitiered magma plumbing beneath Katla volcano, Iceland, *Geochem. Geophys. Geosyst.*, 17, 966–980, doi:10.1002/2015GC006118.

Received 28 SEP 2015

Accepted 14 FEB 2016

Accepted article online 17 FEB 2016

Published online 18 MAR 2016

Abstract Recent seismic unrest and a persistent Holocene eruption record at Katla volcano, Iceland indicate that a near-future eruption is possible. Previous petrological investigations suggest that Katla is supplied by a simple plumbing system that delivers magma directly from depth, while seismic and geodetic data also point toward the existence of upper-crustal magma storage. To characterize Katla's recent plumbing system, we established mineral-melt equilibrium crystallization pressures from four age-constrained Katla tephras spanning from 8 kyr BP to 1918. The results point to persistent shallow- (≤ 8 km depth) as well as deep-crustal (ca. 10 – 25 km depth) magma storage beneath Katla throughout the last 8 kyr. The presence of multiple magma storage regions implies that mafic magma from the deeper reservoir system may become gas-rich during ascent and storage in the shallow crust and erupt explosively. Alternatively, it might intersect evolved magma pockets in the shallow-level storage region, and so increase the potential for explosive mixed-magma ash eruptions.

1. Introduction

Katla is likely one of northern Europe's most active and hazardous volcanic systems as it is ice-covered and displays a very high Holocene eruption frequency with common explosive activity. Studies of Katla's eruptive record have identified >200 Holocene tephra layers that erupted over the last 8.4 kyr, with an average of one event every 48 years in historical time [Óladóttir *et al.*, 2005, 2008]. The last major eruption that pierced the ice surface occurred in 1918, i.e., almost 100 years ago, but unrest and ice melting in 1955 and 1999 might have related to small, subglacial eruptions also [Einarsson and Brandsdóttir 2000]. As Katla and neighbouring Eyjafjallajökull appear to be linked in their eruptive cycles, such that both volcanoes erupted in e.g., 1612 and in 1823 [Sturkell *et al.*, 2008, 2010], the 2010 Eyjafjallajökull eruption might signal that we also need to prepare for a near-future Katla event. A central question for forecasting future eruptive behavior at Katla is the state of the current magma supply system, which will likely be a key control on the size and nature of future eruptive events.

2. Geological Background

Katla volcano, in South Iceland, is part of the propagating Eastern Volcanic Zone (EVZ) of central and south Iceland (Figure 1). The Katla volcanic system has been active for at least a hundred thousand years, and the oldest recorded activity dates to approximately 77,500 years BP [Björnsson *et al.*, 2000]. The Mýrdalsjökull glacier covers Katla's 100 km² ice-filled summit caldera with an average thickness of 230 m [Björnsson *et al.*, 2000; Óladóttir *et al.*, 2008], but Katla's Holocene extra-caldera tephra layers and lava flows record an eruption frequency of between ten and 30 events per millennium for the last 8.4 kyr [Óladóttir *et al.*, 2008]. The Sólheimar ignimbrite of ~12 kyr BP is the largest known silicic eruption from Katla (approximately 7 km³ of erupted material), and it is discussed as the source of the regionally widespread North Atlantic Vedde Ash [Lacasse *et al.*, 1995]. However, only around 12 silicic eruptions, dated at between 6600 and 1675 yr BP, are documented during the Holocene (known as SILK events). These SILK events produced very limited eruptive volumes only, ranging between ~0.01 and ~0.3 km³ of dacitic to rhyolitic tephra per event [Larsen *et al.*, 2001]. In contrast, basaltic volcanism dominated throughout the Holocene, and ~200 basaltic eruptions are recorded for the last 8.4 kyr, which produced between ~0.02 and 1.5 km³ of basaltic tephra individually [Larsen, 2000]. The largest known historical eruption tied to the Katla system is the Eldgjá Fires of 934 AD,

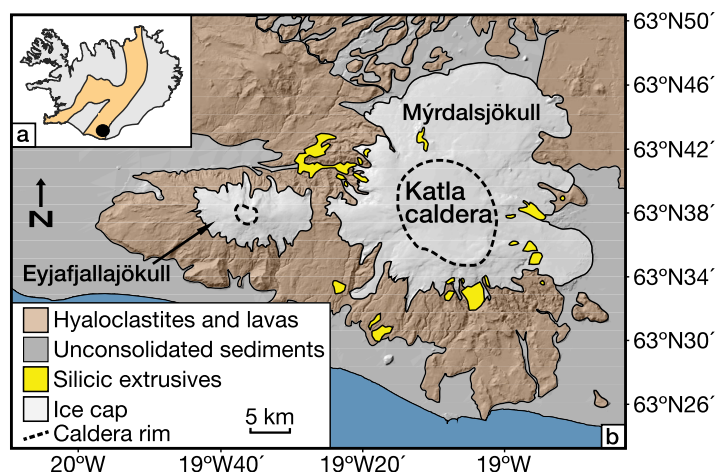


Figure 1. (a) Iceland, with the active volcanic zone, the surface expression of the Mid-Atlantic Ridge, marked in yellow. Black dot marks the location of Katla volcano. (b) Simplified geological map of Katla volcano. The volcano is overlain by the Myrdalsjökull icecap, and Eyjafjallajökull volcano is situated ~25 km to the west.

with a discharge of up to $300,000 \text{ m}^3 \text{ s}^{-1}$ was triggered and between 0.7 and 1 km^3 of tephra was ejected from the volcano [Larsen, 2000; Sturkell et al., 2010; Biass et al., 2014]. Since 1955 the volcano exhibited a near-constant source of seismic activity, with intense inflation of the summit caldera measured by GPS from 1999 to 2004 [Sturkell et al., 2008, 2010]. The last significant unrest at Katla occurred in 2011 when an earthquake swarm was measured and a small jökulhlaup originated from the Myrdalsjökull glacier. Importantly, in addition to the explosive nature of both the basaltic and the silicic eruptions, and the potential of mixed basaltic-silicic eruptions, the presence of the Myrdalsjökull glacier atop the Katla caldera leads to frequent phreatomagmatic phenomena and associated ash-rich events, which have recently been discussed as a potent mechanism for triggering previous climate change in the North Atlantic region [e.g., Jolley and Widdowson, 2005].

3. Current State of Knowledge

Geodetic and seismic investigations identify a shallow-level deformation source and a domain of low seismic wave velocity within the Katla edifice that appears to cause active uplift of portions of the summit caldera [Gudmundsson et al., 1994; Sturkell and Sigmundsson, 2003]. Although glacier movements are complicating the interpretation of volcano deformation and seismic unrest at Katla, seasonal geothermal meltwater release from the volcano indicates a system sensitive to changes in glacial overburden [Wynn et al., 2015], and earthquake activity shows a clear seasonal correlation [Einarsson and Brandsdóttir 2000]. The deeper seismicity ($>3 \text{ km}$) is, in turn, considered to reflect a shallow, and possibly partly silicic magma reservoir or pockets beneath the volcano's summit, which is further supported by the presence of rhyolitic nunataks protruding the icecap over the Katla caldera [Jónsson and Kristjánsson, 2000; Soosalu et al., 2006; Jonsdóttir et al., 2007; Sturkell et al., 2008, 2010]. Previous petrological studies, however, indicate a simple plumbing system that currently provides the volcano with magma directly from mid- to lower-crustal depth, with no evidence for a present-day shallow-level magma reservoir recorded [Óladóttir et al., 2005, 2008]. This concept conflicts the geophysical and geodetic constraints on the location of magma storage within Katla (see above) and complicates assessment of future eruptive potential and style. We therefore investigated the magma plumbing system beneath Katla through a mineralogy and thermobarometry approach on over 1500 single analysis points from pyroxene, feldspar, and glass from four basaltic tephra samples that span the last 8 kyr. These new data were carefully compiled and rigorously tested to exclusively reflect mineral compositions in equilibrium with the final crystallizing melt. We then integrate these new data into the framework of existing geological and petrological data from Katla volcano and develop a petrological model for the basaltic plumbing system beneath Katla.

which produced $>19 \text{ km}^3$ of basalt lava from a fissure north-east of Katla [Thordarson et al., 2001]. The Eldgjá eruption falls between the two youngest tephra layers analyzed in our study. Since the Eldgjá event, there have been approximately 15 eruptions from the Katla caldera, including the notable events of 1755 and 1823, which lasted 120 and 28 days, respectively [Larsen, 2000]. The most recent subaerial eruption at Katla occurred in 1918. This eruption lasted 24 days and generated an eruption column that reached $\sim 14 \text{ km}$ in height. During the eruption, a jökulhlaup (a glacial outburst)

Specifically, petrological and geochemical data available from Katla comprise young lavas, pyroclastic rocks, and tephra layers that span the last ~ 8 kyr [Lacasse *et al.*, 2007; Óladóttir *et al.*, 2008]. These previous investigations established that partial melting of hydrated Icelandic crust was likely a factor in the generation of the silicic materials [Lacasse *et al.*, 2007], which hints at the possibility of shallow silicic magma storage [cf. Zierenberg *et al.*, 2012]. In addition, evolution of Katla's magma supply system is possibly cyclical [Óladóttir *et al.*, 2008] and commenced with a simple plumbing system some 8.4 kyr ago, possibly in the form of a sill and dyke arrangement [Óladóttir *et al.*, 2005, 2008]. A phase of shallow magma storage at 6.8–6.3 kyr ago followed, although no quantification of depth is currently available. The cycle then recommenced with renewed magma storage at depth. These results would point toward a current state of overall simple plumbing for Katla [Óladóttir *et al.*, 2005, 2008], with no significant storage of either basaltic or rhyolitic magmas at shallow levels. In stark contrast, geophysical and geodetic data point to ongoing shallow magma storage at Katla [Jónsson and Kristjánsson, 2000; Soosalu *et al.*, 2006; Jonsdóttir *et al.*, 2007; Sturkell *et al.*, 2008, 2010], which allows for recharge of shallow and possibly silicic magma pockets by ascending basaltic magma. Such mafic injections would likely reactivate the resident magma and perhaps also trigger crustal melting of hydrated basalts, and thus further increase magma volatile content and viscosity, and so promote explosive phenomena via magma mixing as for example seen at Eyjafjallajökull in 2010 [Sigmundsson *et al.*, 2010]. Lastly, the possibility of explosive phenomena is further accentuated by frequent phreatomagmatism from magma-ice interaction due to the presence of the overlying Mýrdalsjökull glacier. To improve our understanding of Katla's magma plumbing system, and to reduce the epistemic uncertainty regarding shallow magma storage at Katla, we have now performed a thermobarometry investigation on basaltic tephra erupted from Katla volcano over the last 8 kyr.

4. Thermobarometry

To constrain the depth of magma storage regions beneath Katla, we employ the clinopyroxene-melt equilibrium thermobarometer from Putirka [2008]. This formulation is based on the jadeite-diopside/hedenbergite exchange equilibria between clinopyroxene and coexisting melt, and is the most accurate amongst available thermobarometers [Mollo *et al.*, 2010]. We also apply the plagioclase-melt equilibrium thermobarometer of Putirka [2005, 2008], and although the standard error for the plagioclase-melt thermobarometer is considerably higher (± 150 MPa for clinopyroxene and ± 247 MPa for plagioclase), a range of petrological studies have recently delivered testable results from these thermobarometers that correlate with information from independent and particularly from geophysical methods [e.g., Barker *et al.*, 2009; Jaxybulatov *et al.*, 2011; Dahren *et al.*, 2012; Weis *et al.*, 2015]. As a final test, we also apply the basaltic glass barometer of Kelley and Barton [2008] to the Katla tephra glass data. This barometer is based on experimentally established phase equilibrium constraints by Yang *et al.* [1996], and is specifically calibrated for basaltic systems and has a SEE of ± 110 MPa.

4.1. Equilibrium Assemblages

As eruptive products are increasingly recognized to carry crystals of variable origins (e.g., pheno-, ante-, and xeno-crysts), it becomes critical to differentiate crystals that grew from the magma they are found in from those picked up from e.g., older intrusive rocks or from unrelated crustal rocks [e.g., Davidson *et al.*, 2005]. To ensure only those mineral compositions that are in equilibrium with the final melt are used in our calculations, we apply rigorous equilibrium tests to the clinopyroxene and feldspar data. The application of an appropriate nominal melt composition is vital to obtain accurate P-T estimates, and is represented by either the groundmass glass, the bulk rock composition, or melt inclusions [e.g., Klügel *et al.*, 2005; Longpré *et al.*, 2008; Dahren *et al.*, 2012]. For equilibrium considerations we avoided targeting melt inclusions as there are (i) issues with preservation of the final equilibrium melt composition [e.g., Baker, 2008] and, (ii) because a crystal and its contained melt inclusions might be in equilibrium with each other, but may still not be linked to the tephra in which the crystal is found. It is therefore fundamental that unsuitable (i.e., unreliable and/or disequilibrium) mineral compositions are identified and rejected before final P-T modeling. Nominal melt compositions tested for mineral-melt equilibrium include EPMA glass and XRF tephra data from this study (supporting information Data Sets 1 and 2) and glass data for these investigated tephra from previous investigations [i.e., Óladóttir *et al.*, 2008].

5. Samples

The three older tephra layers investigated here were collected from a soil profile ca. 25 km east of Katla near the Hólmsá River at Hrífunes, following the sampling procedure of Óladóttir *et al.* [2005]. These three samples have been dated using soil accumulation rate (SAR) that was calibrated by ^{14}C dating to 1250 years BP (1.25 kyr tephra), 4220 years BP (4.22 kyr tephra), and 8000 years BP (8 kyr tephra), and were previously described by Óladóttir *et al.*, [2005, 2008]. A younger tephra sample from the AD 1918 eruption, sampled south of the caldera at Skógasandur, and which was part of the sample set of Lacasse *et al.* [2007], was also investigated. The compositions of these four tephras were established through EPMA glass analysis and comprise essentially transitional alkali basalt (44–48 wt.% SiO_2 ; supporting information Figure S1) [Óladóttir *et al.*, 2008]. The examined tephras are black in colour, generally mineral poor (typically <5% crystal content), and are dominated by a glassy (sideromelane to tachylite) groundmass. The main phenocrysts present are pyroxene, plagioclase, and olivine, which range in size from 30 to 250 μm across (Figure 2). The tephra grains are blocky and highly fragmented, and are overall poorly vesiculated. The brittle fragmentation features observed on several tephra grains suggest magma-water interaction may have played a role as a mechanism for ash generation [cf. Clarke *et al.*, 2009; Liu *et al.*, 2015]. Although no sulphur data are available for the tephras analyzed in this study, Óladóttir *et al.* [2007] measured sulphur concentrations in Katla basaltic tephra layers over the last 8.4 kyr. These analyses revealed concentrations within the “phreatomagmatic range” (600–1600 ppm) following the reasoning of Owen *et al.* [2013], where magma-water interaction and explosive fragmentation is recorded by incomplete sulphur degassing of the tephras [see Óladóttir *et al.*, 2007].

6. Methods

6.1. EPMA Analytical Procedure

Mineral grains of pyroxene and feldspar from the tephras, along with associated glass, were mounted using an epoxy resin, before being attached to glass slides and polished into thin sections. These were carbon coated prior to analysis to minimize charging. Mineral chemistry data were acquired using the field-emission source JEOL JXA-8530F Hyperprobe (FEG-EPMA) at CEMPEG (Centre for Experimental Mineralogy, Petrology and Geochemistry), Uppsala University, Sweden. The run conditions were 15 kV accelerating voltage and 10 nA probe current with 10 s on peak and 5 s on lower and upper background. As textural zoning is not pronounced in the Katla tephra minerals, EPMA analysis targeted the centre of crystals, with a beam width of 1 μm for pyroxene, 3 μm for feldspar, and 10 μm for glass analyses. The following standards were used for calibration; fayalite for Fe, magnesium oxide (MgO) for Mg, pyrophanite (MnTiO_3) for Mn and Ti, aluminium oxide (Al_2O_3) for Al, wollastonite (CaSiO_3) for Ca and Si, chromium oxide (Cr_2O_3) for Cr, nickel oxide (NiO) for Ni, and albite ($\text{NaAlSi}_3\text{O}_8$), orthoclase (KAlSi_3O_8) and apatite ($\text{Ca}_5(\text{PO}_4)_3(\text{OH},\text{F},\text{Cl})$) for Na, K and P, respectively. Major elements have estimated uncertainties of $\leq 1.5\%$ s.d. Further information on analytical precision is given in Barker *et al.* [2015].

6.2. Thermobarometric Modeling

We employed the clinopyroxene-melt equilibrium thermobarometer after Putirka [2008] due to the relative abundance of clinopyroxene in the analyzed tephras. We applied equation (30) and (33) of this formulation, which we label here as CPX08. Sufficient plagioclase is also present for the application of the plagioclase-melt equilibrium thermobarometer [Putirka, 2008, equations (24a) and (25a)], which is based on Putirka [2005] and therefore labeled here as PLAG05.

Common to both thermobarometers are stringent equilibrium test procedures to obtain the best fit equilibrium mineral-melt assemblage. The equilibrium distribution coefficient for Fe-Mg exchange is employed at the first stage of testing for the CPX08 thermobarometer. The test compares the $K_d[\text{FeMg}]$ between clinopyroxene and various melts. Values falling between a K_d of 0.28 ± 0.08 are considered to satisfy equilibrium conditions and are suitable for further use in the thermobarometric models [Duke, 1976; Putirka, 2008]. Values outside of this range are discarded.

Validity of equilibrium conditions between clinopyroxene and the host melt is further tested by plotting the observed mineral components (OMC) of diopside and hedenbergite against the predicted mineral components (PMC) that would crystallize from a given melt [Putirka, 1999, 2008]. Data filtering consists of

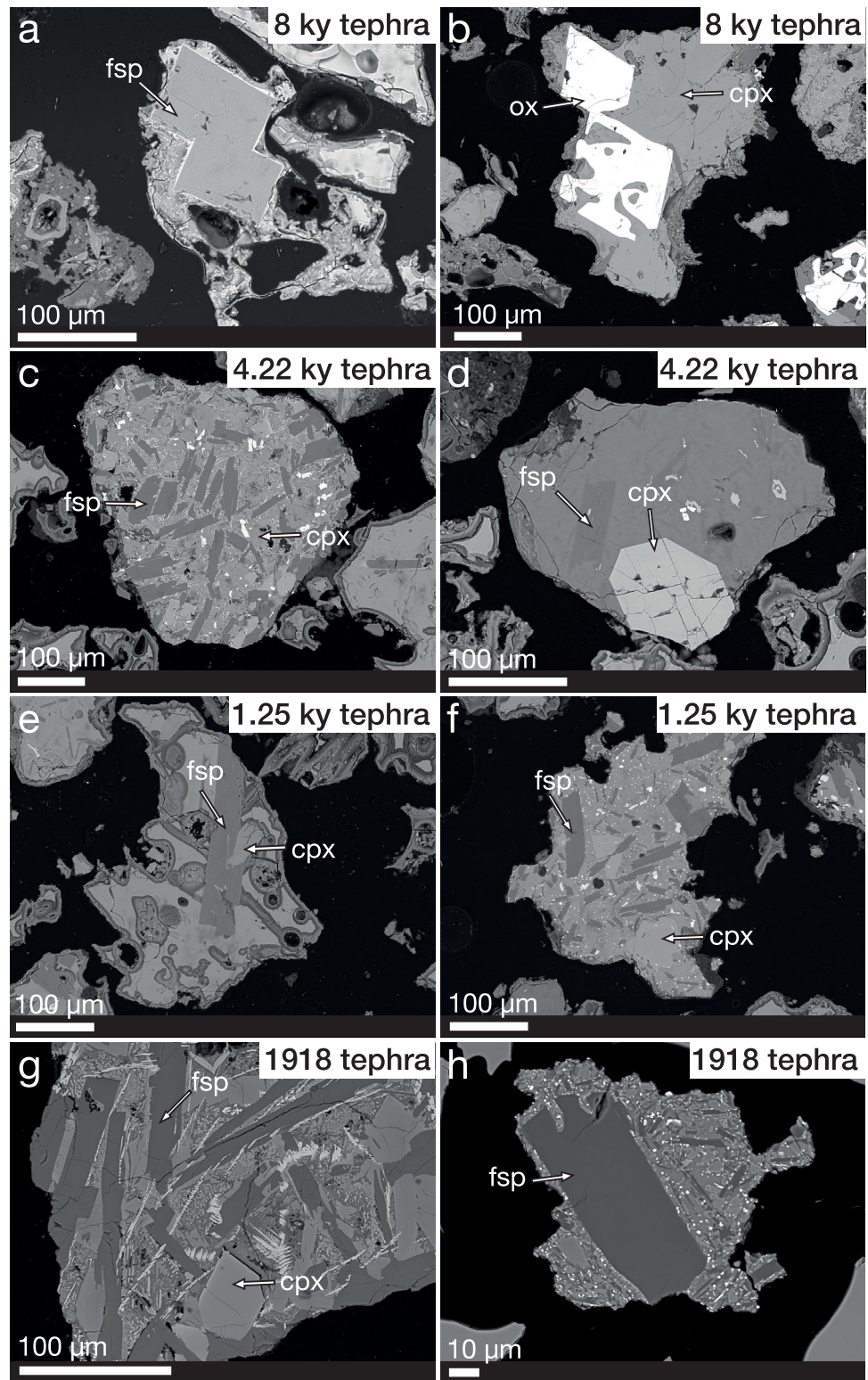


Figure 2. Representative back-scatter electron images of the investigated Katla tephra (8 kyr to 1918 AD). Minerals comprise mainly clino-pyroxene (cpx), plagioclase feldspar (fsp) and Fe-Ti oxides (ox), which occur in clusters and as free-floating crystals within the glassy groundmass.

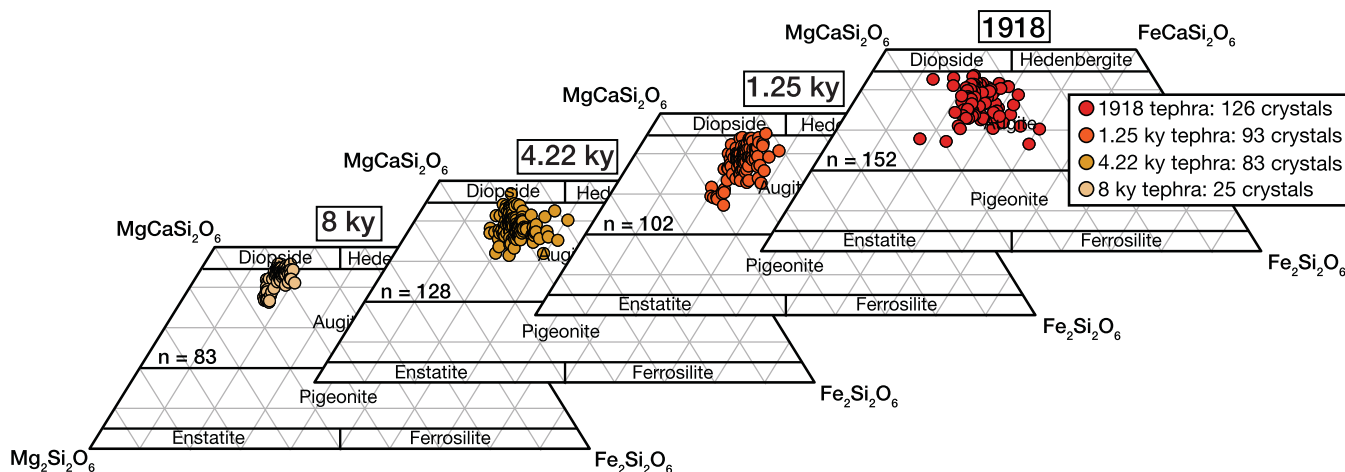


Figure 3. Compositional data from the analyzed Katla tephras are plotted in the “pyroxene quadrilateral.” Katla pyroxene compositions are confined to the diopside and augite fields for all four of the investigated tephra units.

discarding any data points that fall out of $\pm 15\%$ of a one-to-one match between the observed versus predicted Di-Hd line (Figure 6).

Equilibrium testing for the PLAG05 thermobarometer [Putirka, 2005, 2008] employs the equilibrium distribution coefficient for anorthite-albite exchange, $Kd[An-Ab]^{pl-liq} = 0.27 \pm 0.11$ at $T \geq 1050^\circ\text{C}$, a temperature threshold that is applicable to the basaltic tephras analyzed in this study.

For both barometers, a good correlation is observed between the final pressure data and the equilibrium coefficient ($Kd[FeMg]$ for pyroxene and $Kd[AnAb]$ for plagioclase). Therefore, as a final refinement, we consider only the pressure data within $\pm 1\sigma$ of the average pressure for each tephra sequence, which removes irregular outlier data at either end of the P-T spectrum.

6.3. Preeruptive H_2O Content

The clinopyroxene-melt and the plagioclase-melt thermobarometers require the input of a specific preeruptive H_2O estimate. Measurements of basaltic Icelandic glasses have revealed water concentrations of between 0.1 and 1.02 wt.% [Nichols *et al.*, 2002], which is consistent with the data of Jamtveit *et al.* [2001], who employed IR-spectroscopy to obtain water contents in olivine crystals from the North Atlantic Igneous Province and report a range of 0.1–1 wt.%. Moreover, the chosen value is in line with the results of Kelley and Barton [2008], who determined H_2O values of up to 0.94 wt.% for a range of Icelandic glasses, and also with the data of Wallace [2005] who provides a compilation of volatile data from submarine N-MORB glasses that range from ~ 0.1 to 0.9 wt.% H_2O . Lastly, similar results have been obtained through FTIR-spectroscopy on melt inclusions in phenocrysts from Bárðarbunga basaltic tephra that are comparable in composition to those in the Katla basaltic tephras. These analyses reveal a range in H_2O values of between 0.1 and 0.5 wt.% [Bali *et al.*, 2015]. We therefore employed an H_2O value of 0.5 wt.% for the thermobarometric modeling, which we consider an appropriate midrange value for the given magmatic setting. To test our H_2O input value, we affirmed our choice through application of the hygrometer of Waters and Lange [2015] to our tephra data. This method is based on plagioclase-melt equilibrium pairs and is calibrated for a wide range of melt compositions and requires pressure as well as temperature input, and the model is discussed in more detail in the results section. Finally, we note that variation of the water content between 0 and 1 wt.% does not have a significant effect on the mineral-melt thermobarometry results, i.e., small variations amongst samples would not impact the thermobarometry results in a significant way.

6.4. Bedrock Density

To convert pressure estimates (MPa) into depth (km), we use the weighted mean value of 2800 kg/m^3 for the density of the Icelandic crust beneath Katla [e.g., Keiding and Sigmarsson, 2012]. Crustal thickness on Iceland is highly variable, and ranges from around 15–40 km [see Darbyshire *et al.*, 2000; Allen *et al.*, 2002; Foulger *et al.*, 2003]. No robust estimate is available from around the Katla area and for this study we employ

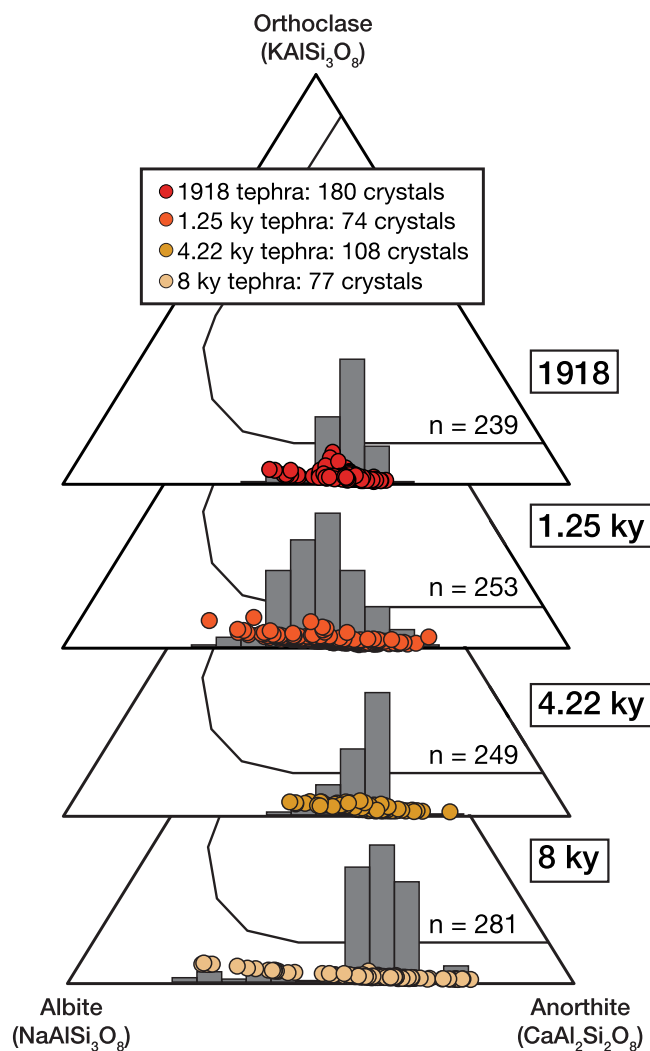


Figure 4. Ternary feldspar diagrams illustrating plagioclase compositions from the four investigated Katla tephra. Frequency distribution of analysis points is superimposed as grey bars behind the compositional data. Data points fall within an anorthite range of An₂₅₋₈₉ and classify the present plagioclase as dominantly bytownite to andesine. Note the considerably tighter cluster of plagioclase compositions for the 1918 sample (see text for details).

spot analyses on 25 crystals from the 8 kyr tephra. Each tephra's average glass composition was considered as the most suitable nominal melt after employing the Kd[FeMg] equilibrium test [cf. Duke, 1976; Putirka, 2008] (Figure 5). Observed versus predicted pyroxene diopside and hedenbergite components were then plotted with the remaining clinopyroxene-melt pairs and only mineral-melt pairs within ±15% of the one-to-one line were taken forward for P-T modeling (Figure 6). For the 1918 tephra, 25% of analyzed data points satisfied all equilibrium tests, while for the 1.25 kyr tephra 35%, for the 4.22 kyr tephra 44%, and for the 8 kyr tephra 63% of crystals satisfy all equilibrium tests. The low percentage of equilibrium pairs returned is a function of the stringent equilibrium testing with age-matched glass compositions. This approach should exclude crystals not directly related to these specific eruptive events (i.e., xenocrysts and/or antecrysts), and provides reliable petrological "time slices" for our investigation (see also below for plagioclase).

The total number of plagioclase analyses comprise (i) 239 spot analyses on 180 crystals from the 1918 tephra, (ii) 253 spot analyses on 74 plagioclase crystals from the 1.25 kyr tephra, (iii) 249 spot analyses on 108 plagioclases from the 4.22 kyr tephra, and (iv) 281 spot analyses on 77 plagioclases from the 8 kyr

a Moho depth of 24 km on the basis of available geodetic data from south-east Iceland [cf. Darbyshire et al., 2000; Allen et al., 2002; Foulger et al., 2003].

7. Results

7.1. Mineral Chemistry

Analyzed clinopyroxenes have a limited compositional range and 98% of the data plot in the augite field. Only ~2% classify as diopside (Figure 3). Significant differences in pyroxene composition between the temporally distinct tephra samples are not observed. Plagioclase crystals from the four tephra samples are usually euhedral and generally lack dendritic quench textures or resorption embayments [cf. Lofgren, 1974]. Plagioclase compositions vary in anorthite content from ~25 to ~89 mol.% for the 1.25 kyr and 8 kyr tephra, but show a slightly more restricted range of ~39 to ~76 mol.% for the 1918 and the 4.22 kyr tephra (Figure 4 and supporting information Data Sets 3 and 4).

7.2. Pressures and Temperatures of Crystallization

Clinopyroxene analyses were quality controlled by selecting only those with sums approaching 100% and with 0 wt.% K₂O. The total number of clinopyroxene analysis points consists of (i) 152 spot analyses on 126 crystals from the 1918 tephra, (ii) 102 spot analyses on 93 crystals from the 1.25 kyr tephra, (iii) 128 spot analyses on 83 crystals from the 4.22 kyr tephra, and (iv) 83

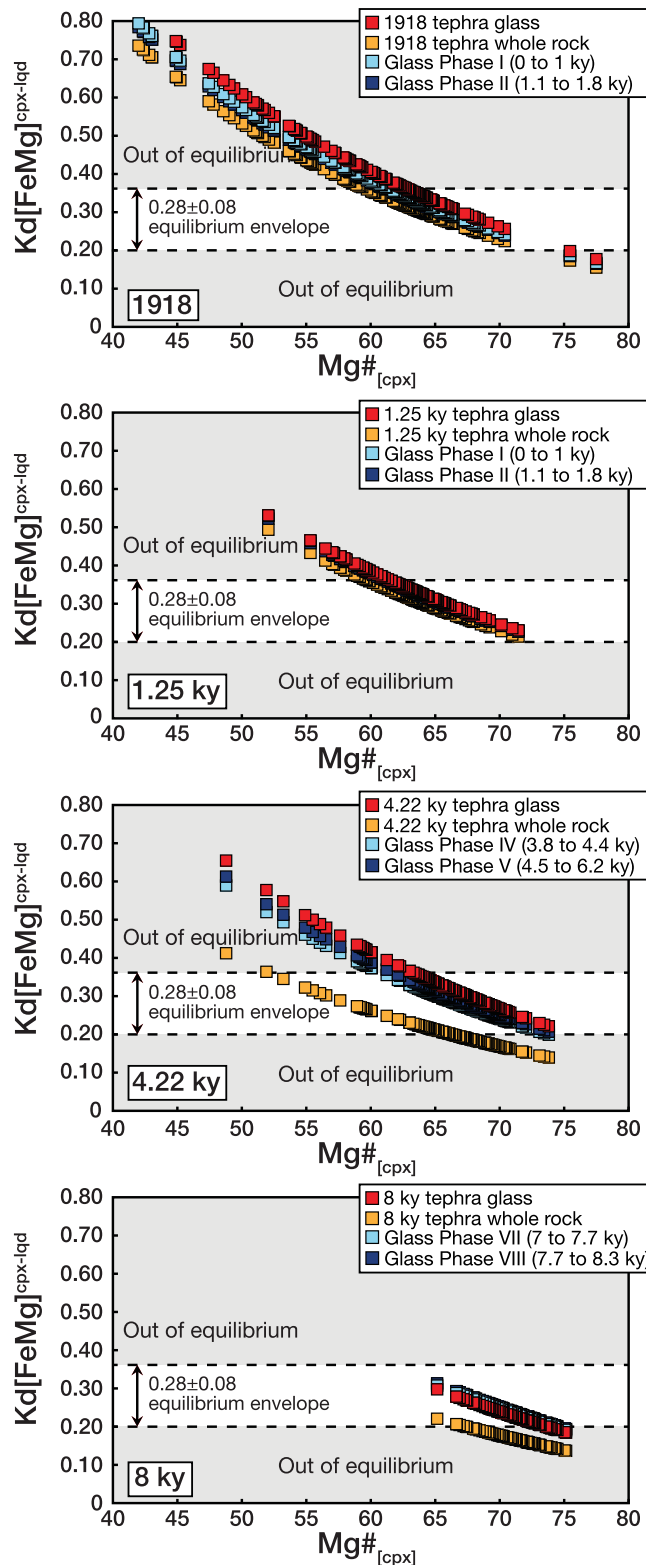


Figure 5. Pyroxene compositions and possible equilibrium melts in a test against $Kd[FeMg] = 0.28 \pm 0.08$ [Duke, 1976; Putirka, 2008]. Data points that fall within this equilibrium envelope are taken to the next level of testing (e.g., Figure 6). The “out of equilibrium” data are discarded at this stage. Note, “Glass Phase” nominal melt data are from Óladóttir et al. [2008].

tephra. The $Kd[An-Ab]$ equilibrium test [Putirka, 2008] (Figure 7) again returned each tephra’s individual glass analysis as the most suitable for the 1918, 4.22 and 8 kyr tephtras, with 21, 30 and 42% of data points satisfying equilibrium conditions (i.e., within a $Kd[An-Ab]^{Pl-liq}$ of 0.27 ± 0.11), respectively. For the 1.25 kyr tephtra, the most suitable nominal melt was, however, the Katla “Phase II” glass (dated at 1.1–1.8 kyr) from Óladóttir et al. [2008], returning 10% of data points within equilibrium. Notably, the An range of all equilibrium plagioclase crystals taken forward for thermobarometric modeling occupies a narrow range of between 58 and 69 mol.%. Lastly, plagioclase saturation surface temperatures were checked to be within the calculated plagioclase temperature ranges, highlighting the suitability of the selected nominal melts (within the model error of $\pm 36^\circ C$) [cf. Putirka, 2008].

Applying a moderate and a slow crystal growth rate of 10^{-12} m/s and 10^{-13} m/s, determined from cooling experiments for plagioclase in basaltic systems [Cashman and Marsh 1988; Cashman, 1990], the largest and smallest plagioclase crystals in the Katla basaltic tephra ($\sim 30 \mu m$ and $250 \mu m$) took between 1 and 80 years to grow. The low crystal content observed in the Katla tephtras is, moreover, typical for prolonged magma storage, where separation of large crystals from the liquid portion of the magma is achieved [Marsh, 2013; Masotta et al., 2013]. The unzoned character of the recorded minerals (pyroxene and plagioclase) furthermore implies a semi-continuous melt supply occurred during growth from e.g., an active crystal mush or from a larger liquid reservoir, or alternatively, that initial zoning was overprinted during prolonged residence [cf. Marsh, 2013]. For these reasons (crystal growth time, low crystallinity, unzoned minerals), we consider our calculated crystallization pressures to reflect magma storage beneath Katla instead of ascent-related conduit processes.

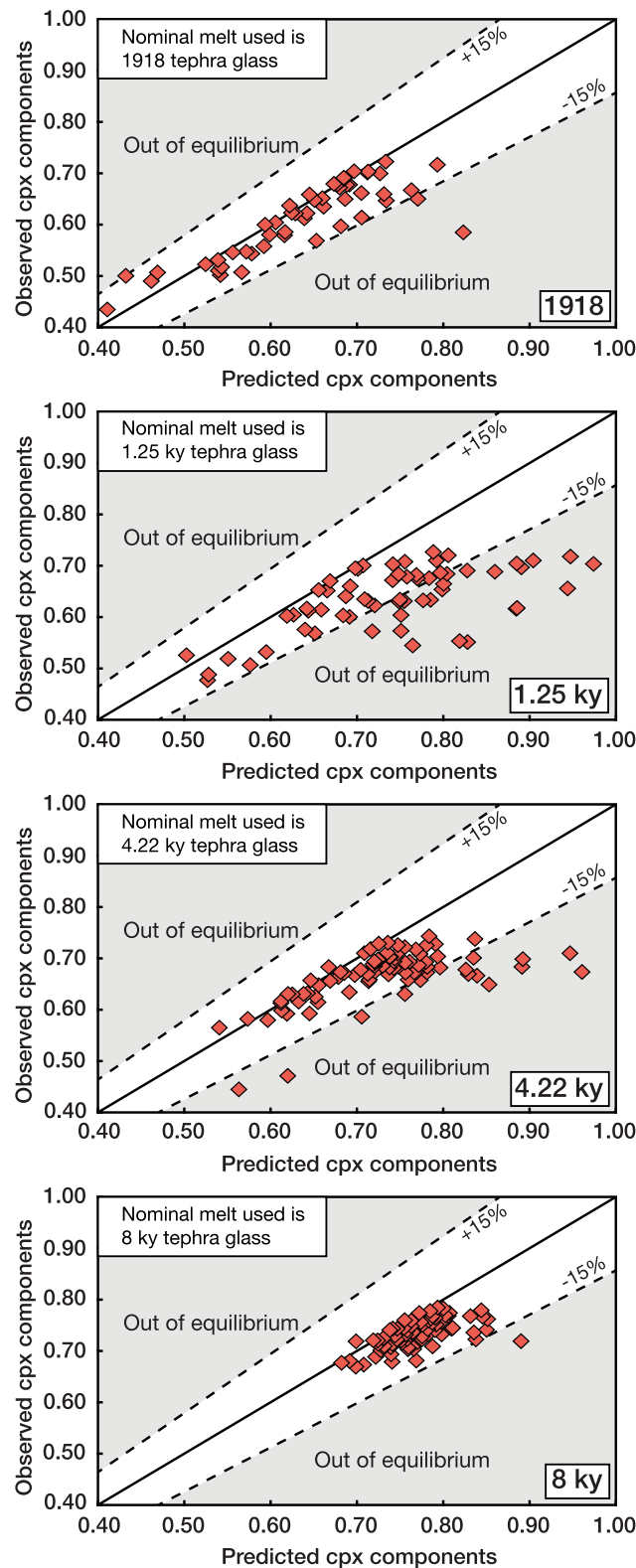


Figure 6. Observed versus predicted mineral components of diopside and hedenbergite for each Katla tephra sequence when paired with the best fit nominal melt. Values that fall within $\pm 15\%$ of the 1:1 line (white areas) satisfy equilibrium conditions and are taken forward for final thermobarometric modeling [cf. Putirka, 1999, 2008].

To ensure high-quality results, we performed plagioclase-liquid hygrometry after Waters and Lange [2015] on our mineral-melt equilibrium pairs, using the mineral and glass compositions and their respective pressure and temperature estimates calculated through plagioclase-melt thermobarometry. The data return an average H_2O estimate of 0.45 ± 0.35 wt.%, which is consistent with our preeruptive H_2O input of 0.5 wt.% used in the thermobarometric modeling (see section 9.3). Calculated clinopyroxene crystallization pressures yield a range from 20 to 961 MPa for the full tephra suite (Figure 8 and Table 1) and the data return persistent mid-crust to sub-Moho crystallization pressures (300–961 MPa, i.e., 10–35 km depth) for over 50% of the data. This depth range is in agreement with our glass barometry modeling for Katla, calculated using the glass barometer of Kelley and Barton [2008], which returns a depth range of between 6 and 33 km for the storage depth of the Katla basalts (Table 1). In addition, these results agree with the data of Neave *et al.* [2013] who derive 8–20 km depth for a clinopyroxene-melt investigation of the 1783 Laki eruption. Notably, the clinopyroxene barometry also records abundant shallow pyroxene crystallization pressures for Katla (≤ 300 MPa), and approximately 40% of pyroxene analyses calculate to below 300 MPa for the three oldest tephra, while only $\sim 3\%$ of data fall below 300 MPa for the 1918 tephra (Figure 9 and Table 1).

Sub-Moho to Moho-level crystallization has frequently been identified through clinopyroxene thermobarometry, e.g., in several oceanic mafic volcanoes (e.g., Cape Verde [Barker *et al.*, 2009]; Gran Canaria [Aulinas *et al.*, 2010]; Tenerife [Longpré *et al.*, 2008]; and La Palma [Galipp *et al.*, 2006]). A likely reason for the Moho-region to be a site of magma storage is the density contrast between mantle and crustal rocks at this boundary [Hansteen *et al.*, 1998; Barker *et al.*, 2009, 2015]. Beneath Katla, the Moho is estimated at ~ 24 km depth [Darbyshire *et al.*, 2000;

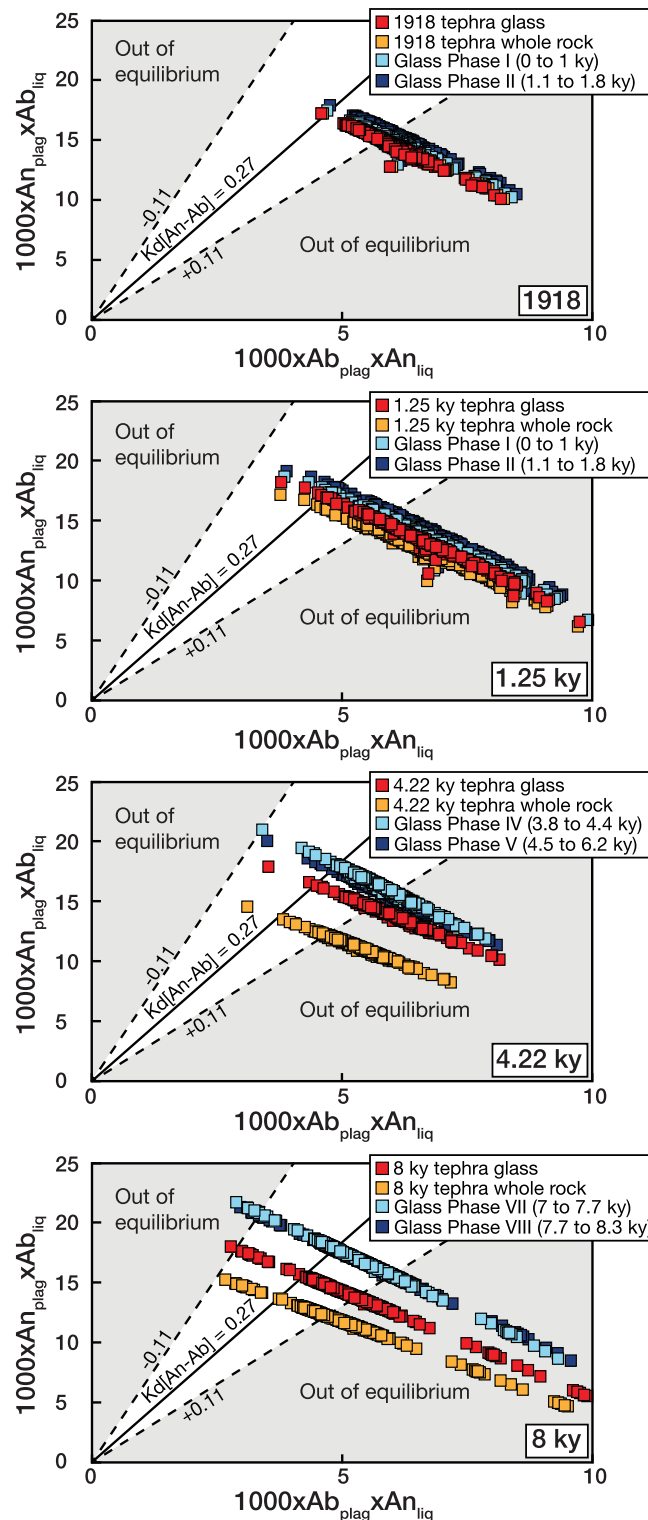


Figure 7. Plagioclase mineral-melt equilibrium test for $Kd[An-Ab] = 0.27 \pm 0.11$ (after Putirka [2008]), using the same range of nominal melts as for the clinopyroxene equilibrium tests in Figure 5. Data points that satisfy equilibrium conditions (i.e., that fall into the white equilibrium envelope) are taken further for thermobarometric modeling. Nonequilibrium data are discarded at that stage.

Allen et al., 2002; Foulger et al., 2003], and our data record extensive crystallization within ± 10 km of this level. Remarkably, the crystallization recorded around the Moho in the 1918 tephra is more disperse relative to the narrower ranges recorded in the earlier tephtras. This disperse and in part deeper crystallization implies that stalling and storage of magma at the Moho level appears to become less focussed with time. This may reflect “flushing” of the magma system during the 934 AD Eldgjá event and subsequent readjustment and refilling from depth, or alternatively, a gradual reduction in density contrast between lower crust and the mantle beneath Katla. Indeed, at this boundary, long-lived magmatic activity ($>10,000$ years) may have progressively changed the lower crust toward an increasingly gabbroic composition.

Calculated plagioclase-melt thermometry crystallization temperatures occupy a narrow range of 1117–1126°C for all tephtras. As a further check on the validity of the temperature results, we apply the Thy et al. [2009] empirical calibration between liquidus temperature and plagioclase An content. Employing the average An content of equilibrium plagioclase from all tephtras of 62 mol.%, a temperature of 1122°C is calculated, which overlaps within the temperature results we obtained through plagioclase-melt thermometry. Crystallization pressures for the Katla tephtras calculated with the plagioclase thermobarometer yield an exclusively shallow pressure range from 84 to 248 MPa (2.5–8 km) and thus constrain plagioclase crystallization to the very upper crust (Figure 8 and Table 1). These low-pressure results overlap with the shallow crystallization pressures derived from a fraction of the clinopyroxene-derived pressure estimates ($\sim 40\%$) in the older Katla tephtras of this study, while only 3% of the pyroxene in the 1918 tephtra is shallow grown (<300 MPa) (Figure 9). The shallow pressures recorded by plagioclase in all analyzed tephtras, including

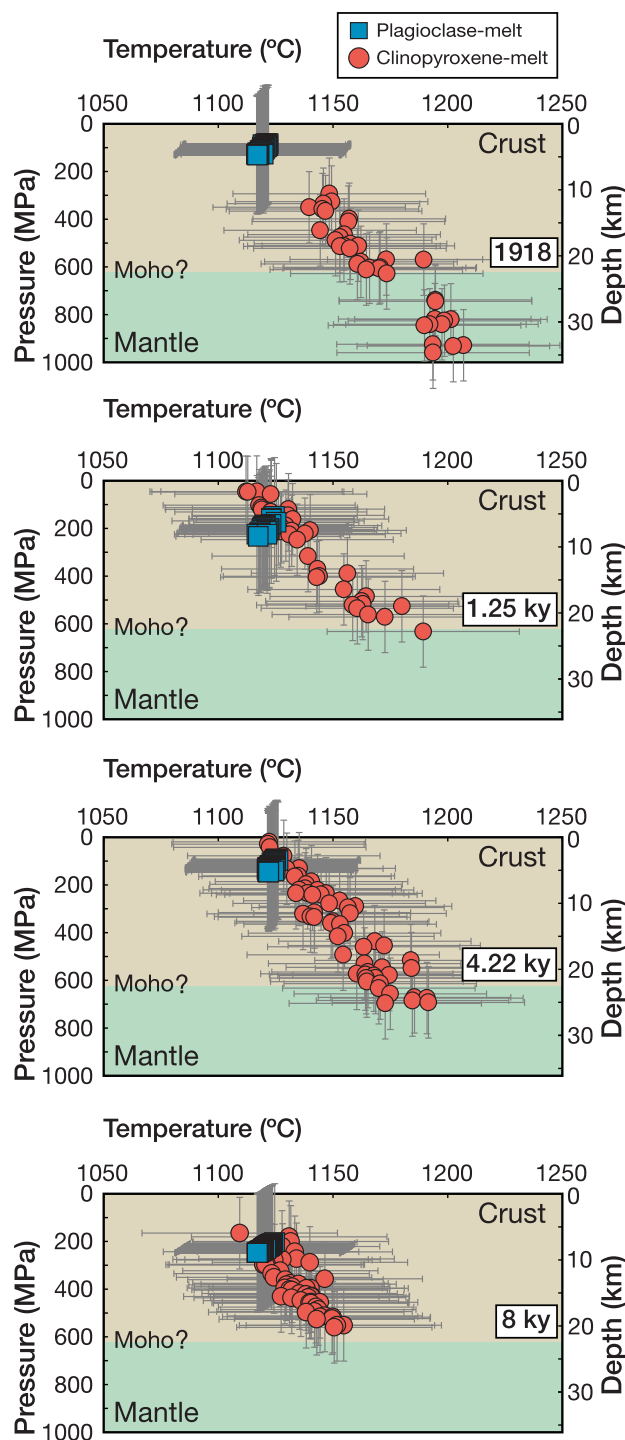


Figure 8. Clinopyroxene- (CPX08) and plagioclase-melt (PLAG05) equilibrium thermobarometry models [Putirka, 2005, 2008] for a magma H_2O content of 0.5 wt.%. Clinopyroxene barometry derives a pressure range from 20 to 961 MPa (red symbols), implying crystallization levels that extend from upper mantle to shallow crustal depths. Note the concurrent decrease in crystallization temperature with decreasing pressure for the pyroxene data, likely indicating heat loss on ascent and storage. The standard error of estimate (SEE) of CPX08 is ± 150 MPa and $\pm 42^\circ\text{C}$. Results from plagioclase thermobarometry (blue symbols) yield crystallization pressures of 84–248 MPa, which are lower than most of the clinopyroxene data, and are confined to the upper crust. The SEE for this thermobarometer is ± 247 MPa and $\pm 36^\circ\text{C}$ (see text for details).

the 1918 tephra, point to ongoing mid-to shallow-crustal storage in addition to a deep reservoir beneath Katla. This realization is consistent with geophysical data that imply current magma residence at shallow levels beneath Katla volcano. Specifically, a low-velocity zone of seismic waves down to a maximum depth of ~ 5 km is present and geodetic models moreover imply an active deformation source within the upper 5 km beneath Katla caldera [Gudmundsson *et al.*, 1994; Jónsson and Kristjánsson, 2000; Soosalu *et al.*, 2006; Jonsdóttir *et al.*, 2007; Sturkell *et al.*, 2008, 2010].

To further assess if there have been temporal changes in Katla's magma plumbing system, we note that (i) the 8 kyr tephra averages at 8 km (228 MPa), (ii) the 4.22 kyr tephra at 4 km (123 MPa), (iii) the 1.25 kyr tephra at 7 km (200 MPa), and (iv) the 1918 tephra averages at 4 km depth (110 MPa) for their plagioclase crystallization depths. These average crystallization depths overlap within the standard error of this barometer (± 247 MPa), which probably implies a persistent shallow storage component within the Katla plumbing system over the last ~ 8 kyr. Mineral assemblages that form by the regular order of crystallization for tholeiitic to mildly alkaline magmas will generally see olivine and clinopyroxene crystallizing before plagioclase joins the crystallizing assemblage [e.g., Winpenny and MacLennan, 2011] and so pyroxene will likely start to form deeper in the crust than plagioclase, but would likely have co-crystallized with plagioclase at shallow levels. Although we did not detect a deep plagioclase fraction, the possibility exists that deeper plagioclase growth is not represented amongst the erupted mineral assemblage, especially as the recorded results emphasize polybaric ascent of Katla magmas over at least the last 8 kyr (Figure 9).

8. Discussion

Our data for the last 8 kyr thus imply that lower- and simultaneous upper-

Table 1. Average Pressure-Temperature-Depth Data From Mineral-Melt and Glass Thermobarometry for the Investigated Katla Tephra^a

	8 kyr Tephra	4.22 kyr Tephra	1.25 kyr Tephra	1918 Tephra
<i>CPX08 Thermobarometer</i>				
Temperature	1135°C ($\sigma = 10$)	1155°C ($\sigma = 18$)	1140°C ($\sigma = 20$)	1170°C ($\sigma = 21$)
Pressure	391 MPa ($\sigma = 103$)	386 MPa ($\sigma = 195$)	289 MPa ($\sigma = 181$)	602 MPa ($\sigma = 196$)
Depth	14 km ($\sigma = 4$)	14 km ($\sigma = 7$)	11 km ($\sigma = 7$)	22 km ($\sigma = 7$)
<i>PLAG05 Thermobarometer</i>				
Temperature	1121°C ($\sigma = 2$)	1123°C ($\sigma = 1$)	1121°C ($\sigma = 2$)	1119°C ($\sigma = 1$)
Pressure	228 MPa ($\sigma = 11$)	123 MPa ($\sigma = 14$)	200 MPa ($\sigma = 21$)	110 MPa ($\sigma = 16$)
Depth	8 km ($\sigma = 0.4$)	4 km ($\sigma = 0.5$)	7 km ($\sigma = 0.8$)	4 km ($\sigma = 0.6$)
<i>Kelley and Barton [2008] Glass Barometer</i>				
Pressure	288 MPa ($\sigma = 54$)	391 MPa ($\sigma = 153$)	395 MPa ($\sigma = 87$)	284 MPa ($\sigma = 56$)

^aStandard error of estimate (SEE) for the clinopyroxene-melt model is $\pm 42^\circ\text{C}$ and ± 150 MPa, and for the plagioclase-melt model $\pm 36^\circ\text{C}$ and ± 247 MPa [Putirka, 2008]. Uncertainty for the glass barometer of Kelley and Barton [2008] is ± 110 MPa.

crustal magma storage may have been a temporally persistent phenomenon at Katla over at least the last 8 kyr. Our results therefore confirm the existence of the previously proposed deep magma storage system below present-day Katla [Óladóttir *et al.*, 2008]. Our data additionally identify shallow-level magma storage in the upper crust during the 8 kyr time span represented by the four tephra time slices we have investigated. Interestingly, the youngest tephra appears to diverge somewhat from the pattern observed in the three older ones, and although the overall plumbing system is similar for the 1918 tephra and the older tephra, the 1918 tephra records deeper and more disperse clinopyroxene crystallization pressures. A progressively reduced density contrast between the lower crust and mantle could be reflected by this data or, alternatively, that the voluminous Eldgjá eruption of 934 AD could have flushed the lower-crustal magma plumbing system which is now refilling from depth. If the more disperse magma storage depths recorded in the 1918 tephra signifies a refilling of the plumbing system after the 934 AD Eldgjá event, a series of future Katla eruptions would appear very likely.

Notably, ascent and intrusion of magma from around Moho levels into upper crustal reservoirs will promote conditions for partial melting of the hydrated basaltic crust ("thermal preconditioning") [cf. Patchett, 1980;

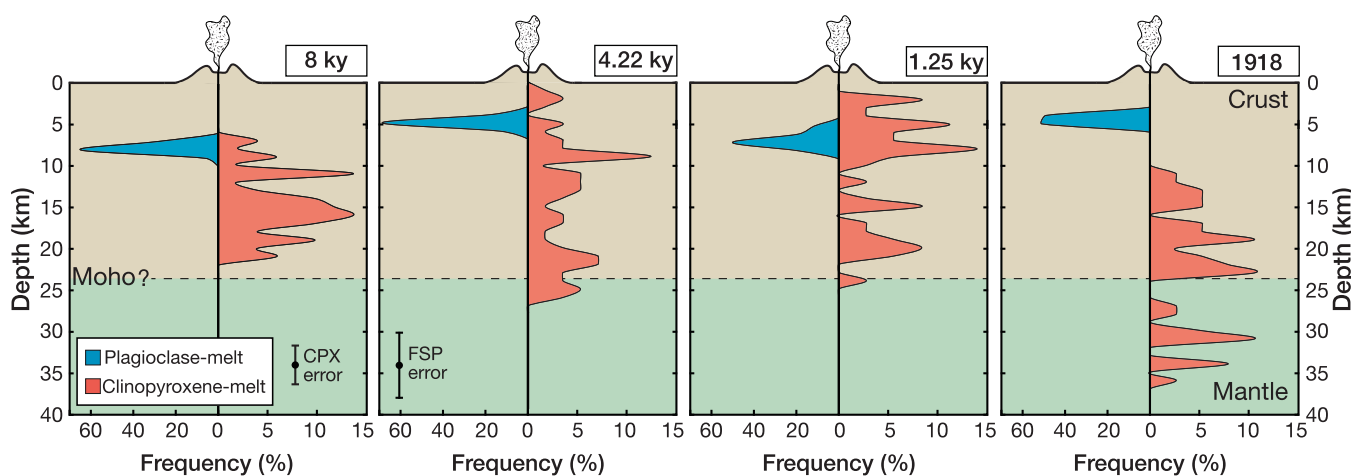


Figure 9. Results of clinopyroxene and plagioclase barometric modeling (after Putirka [2005, 2008]) versus depth. Temporal slices through the Icelandic crust beneath Katla volcano illustrate magma storage at 8, 4.22, and 1.25 kyr BP and in 1918 and indicate a multitiered plumbing system in all four time slices. The data record deep (pyroxene) and shallow-level (pyroxene and plagioclase) magma storage beneath Katla for probably most of the last 8 kyr. The existence of shallow magma pockets increases the likelihood of an Eyjafjallajökull-style eruption at Katla as the shallow storage system may be rapidly reactivated through recharge with mafic magma from depth (see text for details).

Schattel *et al.*, 2014], and is a likely reason for the occasional silicic (SILK) eruptions at Katla [Larsen *et al.*, 2001; Lacasse *et al.*, 2007]. Indeed, the presence of silicic, shallow magma pockets and reservoirs with crustal influence is not uncommon within active central volcanoes in Iceland. At Katla this phenomenon is underlined by actively deforming silicic cryptodomes in the periphery of the caldera. This arrangement is consistent with the recent encounter of a rhyolite magma pocket as shallow as 2 km beneath the Krafla caldera during geothermal exploration drilling [Zierenberg *et al.*, 2012], and with the architecture of fossil magma chambers in eroded caldera volcanoes elsewhere in the North Atlantic Igneous Province [e.g., Burchard *et al.*, 2012; Emeleus and Troll, 2014]. Many shallow sub-caldera storage systems on Iceland likely contain a basaltic heart and peripheral rhyolitic pockets, or cryptodome complexes, which could explain the dominantly basaltic Holocene eruption record at Katla as well as the occasional SILK events [cf. Gudmundsson *et al.*, 1994; Larsen *et al.*, 2001; Soosalu *et al.*, 2006; Lacasse *et al.*, 2007]. Indeed, the probability of magma pockets of e.g., several hundred meters in diameter beneath Katla leads to a high likelihood of interception by thin, but potentially several km long propagating dykes. If silicic pockets in the marginal area of the upper crustal storage region were intersected by rapidly ascending fresh (and hot) mafic magma from e.g., a dyke, magma mixing might result and could act to intensify explosive phreatomagmatic phenomena, such as during the ash-rich explosive phase at Eyjafjallajökull in 2010 [cf. Sparks *et al.*, 1977; Sigmundsson *et al.*, 2010]. In this respect, we note that magma storage beneath Eyjafjallajökull was presumably of a similar configuration to what we postulate for Katla. At Eyjafjallajökull, a storage region at 16–18 km is believed to have fed magma upward to intersect a silicic pocket at <5 km depth, thus initiating the explosive second phase of the 2010 Eyjafjallajökull events [Keiding and Sigmundsson, 2012] (see supporting information Text, supporting information Table S1 and supporting information Figures S2–S4).

9. Concluding Remarks

Within the constraints of the applied thermobarometry methods, our results demonstrate deep- to mid-crustal (≤ 20 km) and simultaneous shallow (≤ 8 km) magma storage beneath Katla. Importantly, our data now reconcile petrochemical observations with geophysical evidence and we must therefore assume that temporally persistent deep and shallow magma reservoirs have existed at Katla over much of the last 8 kyr [cf. Gudmundsson *et al.*, 1994; Jónsson and Kristjánsson, 2000; Sturkell and Sigmundsson, 2003; Soosalu *et al.*, 2006; Jonsdottir *et al.*, 2007; Sturkell *et al.*, 2008, 2010]. The latest plumbing configuration, inferred from the 1918 tephra, may reflect a gradually reduced density contrast at this level, and/or magma build-up from depth after the large Eldgjá fissure eruption in 934 AD. Our new petrological data thus point toward potentially rapid volcanic unrest at Katla, perhaps comparable to e.g., Eyjafjallajökull, due to simultaneous deep and shallow magma storage. The current risk for northern Europe is that either the resident shallow-level magma system at Katla becomes highly evolved through e.g., fractionation or rapid crustal melting (and thus volatile-rich), priming the system for an ash-rich outburst [Owen *et al.*, 2013], or, perhaps more significantly, that mafic replenishments (e.g., via dykes) could intersect silicic parts of the shallow reservoir and trigger a large-volume mixed-magma eruption with a significant silicic component. This scenario would be similar to, but possibly considerably larger than e.g., the 2010 Eyjafjallajökull event, which erupted ~ 0.18 km³ material [Sigmundsson *et al.*, 2010; Gudmundsson *et al.*, 2012; Moune *et al.*, 2012] as opposed to between 0.7 and 1 km³ of tephra that erupted during the phreatomagmatic, but dominantly basaltic, 1918 Katla eruption [Larsen, 2000; Sturkell *et al.*, 2010].

Acknowledgments

We thank B. Óladóttir, L. Thomas and C. Lacasse for providing the tephra samples, and we are grateful to T. Thordarson, M. Masotta, E. Sturkell, A. Tryggvason, Ó. Gudmundsson, F. Sigmundsson, K. Jónsdóttir, V. Smith and O. Sigmundsson for discussions on Katla volcano and its inner workings. We also thank Chenguang Sun and Hugh Tuffen for their insightful reviews, and we are grateful to the Swedish Research Council (VR), the Royal Swedish Academy of Sciences (KVA), and especially the Swedish Centre for Natural Disaster Science (CNS) for financial support. The data for this paper are available in the text, tables, and references therein and from the corresponding author on request.

References

- Allen, R. M., G. Nolet, W. J. Morgan, K. Vogfjörð, M. Nettles, G. Ekström, B. H. Bergsson, P. Erlendsson, G. R. Foulger, and S. Jakobsdóttir (2002), Plume-driven plumbing and crustal formation in Iceland, *J. Geophys. Res.*, *107*(B8), 2163, doi:10.1029/2001JB000584.
- Aulinas, M., D. Gimeno, J. L. Fernandez-Turiel, F. J. Perez-Torrado, A. Rodriguez-Gonzalez, and D. Gasperini (2010), The Plio-Quaternary magmatic feeding system beneath Gran Canaria (Canary Islands, Spain): Constraints from thermobarometric studies, *J. Geol. Soc.*, *167*, 785–801.
- Baker, D. R. (2008), The fidelity of melt inclusions as records of melt composition, *Contrib. Mineral. Petrol.*, *156*, 377–395, doi:10.1007/s00410-008-0291-3.
- Bali, E., O. Sigmundsson, S. Jakobsson, and H. Gunnarsson (2015), Volatile budget of the Nornahraun eruption of the Bárðarbunga system, Iceland, in *Geophysical Research Abstracts, EGU General Assembly 2015*, vol. 17, pp. EGU2015–5757.
- Barker, A. K., P. M. Holm, D. W. Peate, and J. A. Baker (2009), Geochemical stratigraphy of submarine lavas (3–5 Ma) from the Flamengos Valley, Santiago, Southern Cape Verde Islands, *J. Petrol.*, *50*, 169–193, doi:10.1093/ptrology/egn081.
- Barker, A. K., V. R. Troll, J.-C. Carracedo, and P. A. Nicholls (2015), The magma plumbing system for the 1971 Tenguia eruption, La Palma, Canary Islands, *Contrib. Mineral. Petrol.*, *170*(54), 1–21, doi:10.1007/s00410-015-1207-7.
- Biass, S., C. Scaini, C. Bonadonna, A. Folch, K. Smith, and A. Höskuldsson (2014), A multi-scale risk assessment for tephra fallout and airborne concentration from multiple Icelandic volcanoes—Part 1: Hazard assessment, *Nat. Hazards Earth Syst. Sci.*, *14*, 2265–2287.

- Björnsson, H., F. Pálsson, and M. T. Gudmundsson (2000), Surface and bedrock topography of the Mýrdalsjökull ice cap, Iceland: The Katla caldera, eruption sites and routes of jökulhlaups, *Jökull*, *49*, 29–46.
- Burchardt, S., D. Tanner, and M. Krumbholz (2012), The Slaufuradalur pluton, southeast Iceland—An example of shallow magma emplacement by coupled cauldron subsidence and magmatic stoping, *Geol. Soc. Am. Bull.*, *124*, 213–227, doi:10.1130/B30430.1.
- Cashman, K. V. (1990), Textural constraints on the kinetics of crystallization of igneous rocks, *Rev. Mineral.*, *24*, 259–314.
- Cashman, K. V., and B. D. Marsh (1988), Crystal size distribution (CSD) in rocks and the kinetics and dynamics of crystallization, *Contrib. Mineral. Petrol.*, *99*, 292–305.
- Clarke, H., V. R. Troll, and J. C. Carracedo (2009), Phreatomagmatic to Strombolian eruptive activity of basaltic cinder cones: Montana Los Erales, Tenerife, Canary Islands, *J. Volcanol. Geotherm. Res.*, *180*, 225–245, doi:10.1016/j.jvolgeores.2008.11.014.
- Dahren, B., V. R. Troll, U. B. Andersson, J. P. Chadwick, M. F. Gardner, K. Jaxybulatov, and I. Koulakov (2012), Magma plumbing beneath Anak Krakatau volcano, Indonesia: Evidence for multiple magma storage regions, *Contrib. Mineral. Petrol.*, *163*, 631–651, doi:10.1007/s00410-011-0690-8.
- Darbyshire, F. A., R. S. White, and K. F. Priestley (2000), Structure of the crust and uppermost mantle of Iceland from a combined seismic and gravity study, *Earth Planet. Sci. Lett.*, *181*, 409–428, doi:10.1016/S0012-821X(00)00206-5.
- Davidson, J. P., J. M. Hora, J. M. Garrison, and M. A. Dungan (2005), Crustal forensics in arc magmas, *J. Volcanol. Geotherm. Res.*, *140*, 157–170, doi:10.1016/j.jvolgeores.2004.07.019.
- Duke, J. M. (1976), Distribution of the period four transition elements among olivine, calcic clinopyroxene and mafic silicate liquid: Experimental results, *J. Petrol.*, *17*, 499–521, doi:10.1093/petrology/17.4.499.
- Einarsson, P., and B. Brandsdóttir (2000), Earthquakes in the Mýrdalsjökull area, Iceland, 1978–1985; seasonal correlation and connection with volcanoes, *Jökull*, *49*, 59–74.
- Emeleus, C. H., and V. R. Troll (2014), The Rum Igneous Centre, Scotland, *Mineral. Mag.*, *78*, 805–839.
- Foulger, G. R., Z. Du, and B. R. Julian (2003), Icelandic-type crust, *Geophys. J. Int.*, *155*, 567–590, doi:10.1046/j.1365-246X.2003.02056.x.
- Galipp, K., A. Klügel, and T. H. Hansteen (2006), Changing depths of magma fractionation and stagnation during the evolution of an oceanic island volcano: La Palma (Canary Islands), *J. Volcanol. Geotherm. Res.*, *155*, 285–306, doi:10.1016/j.jvolgeores.2006.04.002.
- Gudmundsson, M. T., et al. (2012), Ash generation and distribution from the April–May 2010 eruption of Eyjafjallajökull, Iceland, *Sci. Rep.*, *2*, 572, doi:10.1038/srep00572.
- Gudmundsson, O., B. Brandsdóttir, W. Menke, and G. E. Sigvaldason (1994), The crustal magma chamber of the Katla volcano in south Iceland revealed by 2-D seismic undershooting, *Geophys. J. Int.*, *119*, 277–296, doi:10.1111/j.1365-246X.1994.tb00928.x.
- Hansteen, T. H., A. Klügel, and H.-U. Schmincke (1998), Multi-stage magma ascent beneath the Canary Islands: Evidence from fluid inclusions, *Contrib. Mineral. Petrol.*, *132*, 48–64, doi:10.1007/s004100050404.
- Jamtveit, B., R. Brooker, K. Brooks, L. Larsen, and T. Pedersen (2001), The water content of olivines from the North Atlantic Volcanic Province, *Earth Planet. Sci. Lett.*, *186*, 401–415.
- Jaxybulatov, K., I. Koulakov, M. I. Seht, K. Klinge, C. Reichert, B. Dahren, and V. R. Troll (2011), Evidence for high fluid/melt content beneath Krakatau volcano (Indonesia) from local earthquake tomography, *J. Volcanol. Geotherm. Res.*, *206*, 96–105, doi:10.1016/j.jvolgeores.2011.06.009.
- Jolley, D. W., and M. Widdowson (2005), Did Paleogene North Atlantic rift-related eruptions drive early Eocene climate cooling?, *Lithos*, *79*, 355–366, doi:10.1016/j.lithos.2004.09.007.
- Jonsdóttir, K., A. Tryggvason, R. Roberts, B. Lund, H. Soosalu, and R. Bödvarsson (2007), Habits of a glacier-covered volcano: Seismicity patterns and velocity structure of Katla volcano, Iceland, *Ann. Glaciol.*, *1*, 169–177.
- Jónsson, G., and L. Kristjánsson (2000), Aeromagnetic measurements over Mýrdalsjökull and vicinity, *Jökull*, *49*, 47–58.
- Keiding, J. K., and O. Sigmarsson (2012), Geothermobarometry of the 2010 Eyjafjallajökull eruption: New constraints on Icelandic magma plumbing systems, *J. Geophys. Res.*, *117*, B00C09, doi:10.1029/2011JB008829.
- Kelley, D. F., and M. Barton (2008), Pressures of crystallization of Icelandic magmas, *J. Petrol.*, *49*, 465–492, doi:10.1093/petrology/egm089.
- Klügel, A., T. H., Hansteen, and K. Galipp (2005), Magma storage and underplating beneath Cumbre Vieja volcano, La Palma (Canary Islands), *Earth Planet. Sci. Lett.*, *236*, 211–226, doi:10.1016/j.epsl.2005.04.006.
- Lacasse, C., H. Sigurdsson, H. Johannesson, M. Paterne, and S. Carey (1995), Source of Ash Zone 1 in the North Atlantic, *Bull. Volcanol.*, *57*, 18–32, doi:10.1007/s004450050074.
- Lacasse, C., H. Sigurdsson, S. N. Carey, H. Jóhannesson, L. E. Thomas, and N. W. Rogers (2007), Bimodal volcanism at the Katla subglacial caldera, Iceland: Insight into the geochemistry and petrogenesis of rhyolitic magmas, *Bull. Volcanol.*, *69*, 373–399, doi:10.1007/s00445-006-0082-5.
- Larsen, G. (2000), Holocene eruptions within the Katla volcanic system, south Iceland: Characteristics and environmental impact, *Jökull*, *49*, 1–28.
- Larsen, G., A. Newton, A. Dugmore, and E. Vilmundardóttir (2001), Geochemistry, dispersal, volumes and chronology of Holocene silicic tephra layers from the Katla volcanic system, Iceland, *J. Quat. Sci.*, *16*, 119–132.
- Liu, E. J., K. V. Cashman, A. C. Rust, and S. R. Gislason (2015), The role of bubbles in generating fine ash during hydromagmatic eruptions, *Geology*, *43*, 239–243, doi:10.1130/G36336.1.
- Lofgren, G. (1974), An experimental study of plagioclase morphology: Isothermal crystallisation, *Am. J. Sci.*, *274*, 243–273.
- Longpré, M.-A., V. R. Troll, and T. H. Hansteen (2008), Upper mantle magma storage and transport under a Canarian shield-volcano, Tenos, Tenerife (Spain), *J. Geophys. Res.*, *113*, B08203, doi:10.1029/2007JB005422.
- Marsh, B. D. (2013), On some fundamentals of igneous petrology, *Contrib. Mineral. Petrol.*, *166*, 665–690, doi:10.1007/s00410-013-0892-3.
- Masotta, M., S. Mollo, C. Freda, M. Gaeta, and G. Moore (2013), Clinopyroxene–liquid thermometers and barometers specific to alkaline differentiated magmas, *Contrib. Mineral. Petrol.*, *166*, 1545–1561, doi:10.1007/s00410-013-0927-9.
- Mollo, S., P. Del Gaudio, G. Ventura, G. Iezzi, and P. Scarlato (2010), Dependence of clinopyroxene composition on cooling rate in basaltic magmas: Implications for thermobarometry, *Lithos*, *118*, 302–312, doi:10.1016/j.lithos.2010.05.006.
- Moune, S., O. Sigmarsson, P. Schiano, T. Thordarson, and J. K. Keiding (2012), Melt inclusion constraints on the magma source of Eyjafjallajökull 2010 flank eruption, *J. Geophys. Res.*, *117*, B00C07, doi:10.1029/2011JB008718.
- Neave, D. A., E. Passmore, J. MacLennan, G. Fitton, and T. Thordarson (2013), Crystal–melt relationships and the record of deep mixing and crystallization in the AD 1783 Laki Eruption, Iceland, *J. Petrol.*, *54*, 1661–1690, doi:10.1093/petrology/egt027.
- Nichols, A. R. L., M. R. Carroll, and Á. Höskuldsson (2002), Is the Iceland hot spot also wet? Evidence from the water contents of undegassed submarine and subglacial pillow basalts, *Earth Planet. Sci. Lett.*, *202*, 77–87.
- Óladóttir, B. A., G. Larsen, T. Thordarson, and O. Sigmarsson (2005), The Katla volcano S-Iceland: Holocene tephra stratigraphy and eruption frequency, *Jökull*, *55*, 53–74.

- Óladóttir, B. A., T. Thordarson, G. Larsen, and O. Sigmarsson (2007), Survival of the Myrdalsjökull ice cap through the Holocene thermal maximum: Evidence from sulphur contents in Katla tephra layers (Iceland) from the last 8400 years, *Ann. Glaciol.*, *45*, 183–188, doi:10.3189/172756407782282516.
- Óladóttir, B. A., O. Sigmarsson, G. Larsen, and T. Thordarson (2008), Katla volcano, Iceland: Magma composition, dynamics and eruption frequency as recorded by Holocene tephra layers, *Bull. Volcanol.*, *70*, 475–493, doi:10.1007/s00445-007-0150-5.
- Owen, J., H. Tuffen, and D. W. McGarvie (2013), Explosive subglacial rhyolitic eruptions in Iceland are fuelled by high magmatic H₂O and closed-system degassing, *Geology*, *41*, 251–254, doi:10.1130/G33647.1.
- Patchett, P. J. (1980), Thermal effects of basalt on continental crust and crustal contamination of magmas, *Nature*, *283*, 559–561.
- Putirka, K. (1999), Clinopyroxene + liquid equilibria to 100 kbar and 2450 K, *Contrib. Mineral. Petrol.*, *135*, 151–163, doi:10.1007/s004100050503.
- Putirka, K. D. (2005), Igneous thermometers and barometers based on plagioclase + liquid equilibria: Tests of some existing models and new calibrations, *Am. Mineral.*, *90*, 336–346, doi:10.2138/am.2005.1449.
- Putirka, K. D. (2008), Thermometers and barometers for volcanic systems, *Rev. Mineral. Geochem.*, *69*, 61–120, doi:10.2138/rmg.2008.69.3.
- Schattel, N., M. Portnyagin, R. Golowin, K. Hoernle, and I. Bindeman (2014), Contrasting conditions of rift and off-rift silicic magma origin on Iceland, *Geophys. Res. Lett.*, *41*, 5813–5820, doi:10.1002/2014GL060780.
- Sigmundsson, F., et al. (2010), Intrusion triggering of the 2010 Eyjafjallajökull explosive eruption, *Nature*, *468*, 426–30, doi:10.1038/nature09558.
- Soosalu, H., K. Jónsdóttir, and P. Einarsson (2006), Seismicity crisis at the Katla volcano, Iceland—Signs of a cryptodome?, *J. Volcanol. Geotherm. Res.*, *153*, 177–186, doi:10.1016/j.jvolgeores.2005.10.013.
- Sparks, R. S. J., H. Sigurdsson, and L. Wilson (1977), Magma mixing: A mechanism for triggering acid explosive eruptions, *Nature*, *267*, 315–318.
- Sturkell, E., F. Sigmundsson, and P. Einarsson (2003), Recent unrest and magma movements at Eyjafjallajökull and Katla volcanoes, Iceland, *J. Geophys. Res.*, *108*(B8), 2369, doi:10.1029/2001JB000917.
- Sturkell, E., P. Einarsson, M. J. Roberts, H. Geirsson, M. T. Gudmundsson, F. Sigmundsson, V. Pinel, G. B. Guðmundsson, H. Ólafsson, and R. Stefánsson (2008), Seismic and geodetic insights into magma accumulation at Katla subglacial volcano, Iceland: 1999 to 2005, *J. Geophys. Res.*, *113*, B03212, doi:10.1029/2006JB004851.
- Sturkell, E., P. Einarsson, F. Sigmundsson, A. Hooper, B. G. Ofeigsson, H. Geirsson, and H. Olafsson (2010), Katla and Eyjafjallajökull volcanoes, *Dev. Quat. Sci.*, *13*, 5–21.
- Thordarson, T., D. J. Miller, G. Larsen, S. Self, and H. Sigurdsson (2001), New estimates of sulfur degassing and atmospheric mass-loading by the 934 AD Eldgja eruption, Iceland, *J. Volcanol. Geotherm. Res.*, *108*, 33–54.
- Thy, P., C. Tegner, and C. E. Leshner (2009), Liquidus temperatures of the Skaergaard magma, *Am. Mineral.*, *94*, 1371–1376.
- Wallace, P. J. (2005), Volatiles in subduction zone magmas: Concentrations and fluxes based on melt inclusion and volcanic gas data, *J. Volcanol. Geotherm. Res.*, *140*, 217–240, doi:10.1016/j.jvolgeores.2004.07.023.
- Waters, L. E., and R. A. Lange (2015), An updated calibration of the plagioclase-liquid hygrometer-thermometer applicable to basalts through rhyolites, *Am. Mineral.*, *100*, 2172–2184, doi:10.2138/am-2015-5232.
- Weis, F. A., H. Skogby, V. R. Troll, F. M. Deegan, and B. Dahren (2015), Magmatic water contents determined through clinopyroxene: Examples from the Western Canary Islands, Spain, *Geochem. Geophys. Geosyst.*, *16*, 2127–2146, doi:10.1002/2015GC005800.
- Winpenny, B., and J. Maclennan (2011), A partial record of mixing of mantle melts preserved in Icelandic phenocrysts, *J. Petrol.*, *52*, 1791–1812, doi:10.1093/petrology/egr031.
- Wynn, P. M., D. J. Morrell, H. Tuffen, P. Barker, F. S. Tweed, and R. Burns (2015), Seasonal release of anoxic geothermal meltwater from the Katla volcanic system at Sólheimajökull, Iceland, *Chem. Geol.*, *396*, 228–238, doi:10.1016/j.chemgeo.2014.12.026.
- Yang, H.-J., R. J. Kinzler, and T. L. Grove (1996), Experiments and models of anhydrous, basaltic olivine-plagioclase-augite saturated melts from 0.001 to 10 kbar, *Contrib. Mineral. Petrol.*, *124*, 1–18, doi:10.1007/s004100050169.
- Zierenberg, R. A., et al. (2012), Composition and origin of rhyolite melt intersected by drilling in the Krafla geothermal field, Iceland, *Contrib. Mineral. Petrol.*, *165*, 327–347, doi:10.1007/s00410-012-0811-z.